Ecological Modelling 464 (2022) 109798

Contents lists available at ScienceDirect

Ecological Modelling

journal homepage: www.elsevier.com/locate/ecolmodel

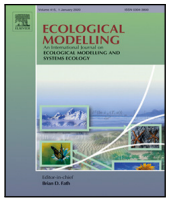

A fine-scale marine mammal movement model for assessing long-term aggregate noise exposure

Ruth Joy [a,b,*], Robert S. Schick [c], Michael Dowd [d], Tetyana Margolina [e], John E. Joseph [e], Len Thomas [f]

[a] School of Environmental Science, Simon Fraser University, 8888 University Drive, Burnaby, BC, V5A 1S6, Canada
[b] SMRU Canada Ltd., Suite 604, 55 Water Street, Vancouver, British Columbia, V6B 1A1, Canada
[c] Marine Geospatial Ecology Lab, Nicholas School of the Environment, Duke University, Box 90328, Durham, NC, 27708, USA
[d] Department of Mathematics and Statistics, Dalhousie University, 6316 Coburg Road, PO Box 15000 Halifax, Nova Scotia, B3H 4R2, Canada
[e] Oceanography Department, Naval Postgraduate School, Monterey, United States
[f] Centre for Research into Ecological and Environmental Modelling, The Observatory, University of St Andrews, KY16 9LZ, United Kingdom

ARTICLE INFO

Keywords:
Animal movement model
Particle filter
Naval sonar
Dose–response function
Aggregate impact
Fin whales

ABSTRACT

Understanding the impacts of anthropogenic sound on marine mammals is important for effective mitigation and management. Sound impacts can cause behavioral changes that lead to displacement from preferred habitat and can have negative influence on vital rates. Here, we develop a movement model to better understand and simulate how whales respond to anthropogenic sound over ecologically meaningful space and time scales. The stochastic model is based on a sequential Monte Carlo sampler (a particle filter). The movement model takes account of vertical dive information and is influenced by the underwater soundscape and the historical whale distribution in the region. In the absence of noise disturbance, the simulator is shown to recover the historical whale distribution in the region. When noise disturbance is incorporated, the whale's behavioral response is determined through a dose–response function dependent on the received level of sound. The aggregate impact is assessed by considering both the duration of foraging loss and the spatial shift to alternate (and potentially less favorable) habitat. Persistence of the behavioral response in time is treated through a 'disruption' parameter. We apply the approach to a population of fin whales whose distribution overlaps naval sonar testing activities beside the Southern California range complex. The simulation shows the consequences of one year of naval sonar disturbance are a function of: i) how loud the sound source is, ii) where the disturbed whales are relative to preferred (high density) habitat, and iii) how long a whale takes before returning to a pre-disturbance state. The movement simulator developed here is a generic movement modeling tool that can be adapted for different species, different regions, and any acoustic disturbances with known impacts on animal populations.

1. Introduction

The US Marine Mammal Protection Act (16 U.S.C. §§1361 et seq.) aims to protect marine mammals from harassment in US waters. Exceptions may be made for certain activities, including those that generate underwater sound. A key example, and a central motivator for this paper, is when tactical sonar is used for naval training and testing. To receive an exception, the US Navy undertakes extensive planning to determine how many whales could be exposed to sonar, and the levels at which each animal is exposed. At present, one limitation of this approach is that each simulation of behavioral effects is done for a 24-hour period, with no memory of previous disturbance. This limits our understanding of longer term effects of multiple sound exposure on whales' behavior, health, and ultimately vital rates. The literature on the link between exposure and impacts on hearing and behavior is rich (e.g., Southall et al., 2019), but determining the aggregate impacts of multiple exposures, as well as the cumulative effect of different stressors on vital rates is an open and pressing research question (National Academies of Sciences, Engineering, and Medicine, 2017).

Animal movement models are a class of stochastic models that simulate trajectories through time and space (Hooten et al., 2017). These stochastic movement models are extremely flexible in terms of character of the realizations of animal movement they can generate. They generally must be confronted with location data (tracks) within an inferential framework in order to provide reasonable simulations

* Corresponding author at: School of Environmental Science, Simon Fraser University, 8888 University Drive, Burnaby, BC, V5A 1S6, Canada.
E-mail address: rjoy@sfu.ca (R. Joy).

https://doi.org/10.1016/j.ecolmodel.2021.109798
Received 14 December 2020; Received in revised form 31 August 2021; Accepted 25 October 2021
Available online 25 November 2021

of actual trajectories. Bio-logging technologies have provided these data, and revolutionalized the study of animal movement (Whitford and Klimley, 2019). Fusion of movement models and tracking data through statistical methods allow for understanding of animal behavior inferred through movement. Approaches often focus on estimating the parameters for behavioral inference (e.g., Patterson et al., 2017) using methods such as Bayesian Markov chain Monte Carlo (MCMC; Morales et al., 2004; Joy et al., 2015), and statistical frameworks such as hidden Markov models (Langrock et al., 2012; Whoriskey et al., 2017), and state space models (Jonsen et al., 2003; Dowd and Joy, 2011). There is also significant interest in developing movement simulators that simulate realistic trajectories but do not rely directly on observed track data. These include the use of potential functions that influence model trajectories based on imposed field of attraction or repulsion (Brillinger, 2010; Preisler et al., 2013). One recent development makes use of resource selection functions that encapsulate habitat preference (Michelot et al., 2019a,b), and proposes an MCMC based simulator wherein the step selection functions, or movement models, are such that the long run distribution tends to the resource selection function. Here, we offer a related but distinct sequential Monte Carlo sampler (Del Moral et al., 2006) for movement simulation that can account for historical distributions of whale abundance, as well as incorporate sound exposure.

A suite of individual-based animal movement models have been developed to merge individual-based movement with exposure to noise disturbance (e.g., AIM: Frankel et al., 2002; SAFESIMM: Donovan et al., 2012; 3MB: Hauser, 2006; and the US Navy Acoustics Effect Model(NAEMO): Blackstock et al., 2018; 3MTSim: Parrott et al., 2011). These existing methods are limited in a number of respects. First, long-run movement in the absence of disturbance does not tend to the resource selection function. Second, none of these acoustic effects models accounts for behavioral context (Ellison et al., 2012), although a few include realistic avoidance behavior (Donovan et al., 2017). Third, existing approaches are limited in their ability to assess aggregate exposure over more ecologically meaningful time frames, i.e., those that may be linked to vital rates and population consequences (e.g., Pirotta et al., 2018). From both a conservation and ecological standpoint, it is important to move beyond single event assessments and examine long-run movement of individuals and how their spatial use changes across multiple sound exposures.

This study proposes a novel formulation for a marine animal movement model, in the form of a particle filter based movement sampler. This is motivated by, and targeted at, a population of fin whales in the coastal waters off southern California, although the methods themselves are quite general. The movement simulator provides a framework for evaluating long term consequences (e.g., over one year) of sound disturbance, by tracking sound exposure and behavioral changes on the individuals, that collectively may induce population level consequences on vital rates. We make use of a multi-scale individual-based random walk marine mammal movement model that simulates horizontal movement and diving over a period of up to one year of US naval sonar exercises with dive-by-dive resolution. The sequential Monte Carlo sampler allows movement trajectories to follow historical whale distributions. In this way, individual-based movement simulations permit us to incorporate the following: (i) the aggregate noise exposure in an area; (ii) the movement of individuals in response to the exposure; and (iii) the changes in habitat-use as a result of those sound-induced behavioral changes. We propose this model as part of a management-focused tool that, when calibrated to local conditions, could be used in combination with existing methods to estimate behavioral effects of accumulated exposure and the distribution of aggregate exposure and behavior response within the population. Collectively, this tool assists on-going efforts to better describe the consequences of anthropogenic sources of disturbance on marine mammals and the possible effect of mitigation measures. While our focus is on marine mammals and underwater sound, our movement modeling approach could be applied to other marine or terrestrial species to study spatial habitat use and behavioral disturbance due to anthropogenic stressors.

2. Methods

We develop a stochastic modeling approach that simulates the movement of a whale through space and time. It is based on a stochastic movement model producing whale trajectories that are influenced by historical whale distribution, as well as underwater noise fields. In this section, we first introduce a general movement model. We consider its vertical dimension as being taken from a population dive distribution. This is coupled to a random walk model of the horizontal movement. Next, we demonstrate how realizations (trajectories) of this stochastic movement model can be guided by a historical spatial whale distribution surface, something that is often available from past studies based on sightings surveys or other data on habitat utilization. Finally, the influence of underwater noise is incorporated using a hypothetical dose–response function to define the probability of a behavioral response that takes the form of an alteration of the movement pathway to avoid or minimize further sound exposure.

The general framework for the movement model is the following stochastic time series model,

$$\boldsymbol{x}_t = d(\boldsymbol{x}_{t-1}, \phi, \epsilon_t) \tag{1}$$

where $\boldsymbol{x}_t$ is the state vector that describes the state at time t, which here represents the animal's location. The operator d steps the movement process forward in time. It is Markovian and has a dependence on the state at the previous time, $\boldsymbol{x}_{t-1}$, as well as on a set of parameters, ϕ. The term ϵ_t represents stochastic forcing or random disturbance; it is generally assumed serially uncorrelated and can enter multiplicatively or additively. The unit time index, and the time increment defined by it, is arbitrary — it could reflect the discretization time used in a numerical scheme for solving differential equations (hence mimicking continuous movement), it could be the time between observations of the system, or it could simply reflect any time interval of interest that is regularly or otherwise spaced. Eq. (1) is a very general movement model, and below it is made application-specific by first considering the movement in the vertical (depth) dimension, and then showing how that informs movement in the horizontal dimension.

2.1. Vertical movement

We first consider the vertical movement or dive characteristics, as this acts to specify many of the features of the horizontal movement. The statistics describing an individual dive typically are assumed to follow a known distribution including dive duration, descent rates, time at the surface between dives, and time at depth (Hauser, 2006). Here, we consider the intermediate time spent not diving as surface related activity that is linked to the previous subsurface component of a dive which relates in part to the recovery phase after submergence (Tyack et al., 2006). This couplet of submergence and surface recovery is henceforth called a 'dive'. Dives are randomly generated from species' dive statistics (or taken directly from dives recorded on tags). Each dive realization is assumed to occur independently from any previous dive, and represents a discrete event. Dive durations are variable, and do not conform to a regular time interval. Furthermore, for realism, each dive is also constrained to be less deep than the local bathymetry at the dive location. Importantly, as outlined below, these realizations of vertical movement are coupled to the horizontal movement with the duration of each dive defining the associated time step for the stochastic model of horizontal movement, as well as the magnitude of the horizontal displacement.

2.2. Horizontal movement

The horizontal part of the movement model is based on a simple 2-D random walk that is straightforward to simulate from:

$$\boldsymbol{x}_t = \boldsymbol{x}_{t-1} + \epsilon_t \qquad \text{where } \epsilon_t \sim \mathcal{N}(0, \sigma_t^2)\ . \tag{2}$$

Here, $\boldsymbol{x}_t$ is a 2×1 vector that represents the northing and easting UTM position of the whale at time step t. The unit time step here is taken as the dive duration, which will be a variable, not constant, length of time. Longer dive durations tend to be associated with larger displacement between two point locations (Fauchald and Tveraa, 2003). To incorporate this feature, we make the variance term σ_t^2 in the state evolution Eq. (2) a scalar function of the dive duration. Specifically, the standard deviation for the displacement, σ_t, is the dive duration multiplied by a typical speed of the whale species under consideration. We further add a constraint to the horizontal movement through a user-defined threshold that rejects a proposed displacement if it exceeds the maximum possible speed of the species, effectively making ϵ_t a normal distribution with its upper tail truncated. Hence, the transition density $p(\boldsymbol{x}_t|\boldsymbol{x}_{t-1})$ associated with Eq. (2) is a truncated normal as described.

2.3. Incorporating spatial habitat use

The basic random walk given by Eq. (2) is, by itself, not a particularly informative or realistic model for whale location. Eq. (2) has no directional fidelity to the movement, meaning that the expected location is the simulation starting position, and location variance just grows as a linear function of time. To add realism through directional preference, we use this movement model within a sequential Monte Carlo sampler to take into account information on historical whale spatial density. Below, we assume we have an estimate of the spatial probability density function of whales in a mapped region from past studies. In practice, this habitat preference is often a product derived from whale sightings fitted with a density surface model or from a species distribution model. It may alternatively be referred to as a resource selection function (Boyce and McDonald, 1999). We will term this quantity the *historical whale spatial density* to emphasize that it is an already obtained quantity, and denote it as $p(\boldsymbol{y}_t|\boldsymbol{x}_t)$. This says that for a particular animal location $\boldsymbol{x}_t$, we can determine the probability of a whale observation, $\boldsymbol{y}_t$, occurring there.

The historical whale spatial density will be used to influence the local trajectory of the random walk, and hence bias the horizontal movement and impart directional fidelity that reflects habitat preference. More specifically, we seek the posterior distribution of the new whale location taking account the previous position, the movement model prediction, and the historical whale spatial density. From Bayes' theorem we have

$$p(\boldsymbol{x}_t|\boldsymbol{y}_t) \propto p(\boldsymbol{y}_t|\boldsymbol{x}_t)\; p(\boldsymbol{x}_t|\boldsymbol{x}_{t-1}) \tag{3}$$

where $p(\boldsymbol{x}_t|\boldsymbol{y}_t)$ is the target distribution. Note that the movement model $p(\boldsymbol{x}_t|\boldsymbol{x}_{t-1})$ and the historical whale spatial density $p(\boldsymbol{y}_t|\boldsymbol{x}_t)$ also provide the components for a state space model whose goal is to determine the posterior $p(\boldsymbol{x}_t|\boldsymbol{y}_t)$ for $t = 1, \ldots, T$. We exploit this fact below to propose a sequential estimation procedure for the state that combines the random walk movement model with the historical whale spatial density in order to generate realizations of whale trajectories that are draws from the posterior. Note that there are no parameters to estimate here since the displacement variance, σ_t^2, and the whale observation density, $p(\boldsymbol{y}_t|\boldsymbol{x}_t)$, are user inputs and hence specified.

Since the distributions considered are generally non-Gaussian, we use the basic particle filtering algorithm of sequential importance resampling (SIR; Gordon et al., 1993; Kitagawa, 1987). In general terms this works as follows. Starting with initial conditions $\boldsymbol{x}_0$, the whale movement model predicts possible movement locations, the historical whale spatial density weights these locations based on the probability of a whale being found there, and a weighted resampling occurs after which a new location is determined. The procedure then continues sequentially forward through time. The particle filter is simple to implement, well understood, and converges to the target posterior (Kitagawa, 1987). Our specific adaption of this sequential Monte Carlo algorithm to generating whale trajectories is given below.

For this sequential, recursive algorithm we assume, without loss of generality, that we are at time $t-1$ and know the whale location at that time (i.e., the location at the start of a dive). Our goal is to determine its position at the next time t (at the end of the dive and after surface recovery). We do this according to the following sequence of steps starting with the whale location $\boldsymbol{x}_{t-1}$:

I. Set up: Determine the displacement variance term, σ_t^2, in the horizontal movement model (2). This is done by randomly generating a dive duration from a species' dive distribution (see Sections 2.1 and 2.2).

II. Prediction: Simulate n possible whale positions at time t by drawing n realizations of the random vector of displacement, ϵ_t, and applying the random walk model (2) to each one. This yields a set of n possible predicted locations, designated $\{\boldsymbol{x}_{t|t-1}^{(i)}\}_{i=1}^{n}$, which is a draw from the transition density $p(\boldsymbol{x}_t|\boldsymbol{x}_{t-1})$. Here, $\boldsymbol{x}_{t|t-1}$ designates the one-step ahead forecast location prior to any consideration of the historical whale spatial density, and the superscript i identifies an ensemble member (particle).

III. Weighting: Calculate a weight for each member of the forecast ensemble, $\{w_t^{(i)}\}$, $i = 1, \ldots, n$. The n weights are calculated for each forecast whale position as being proportional to the whale spatial density,

$$w_t^{(i)} \propto p(\boldsymbol{y}_t|\boldsymbol{x}_{t|t-1}^{(i)}). \tag{4}$$

IV. Selection: A single ensemble member is selected randomly from the candidate set $\{\boldsymbol{x}_{t|t-1}^{(i)}\}_{i=1}^{n}$ with probability proportional to their weights $\{w_t^{(i)}\}$. This becomes the next location in the simulated track at time t, or the value for the position $\boldsymbol{x}_t$.

Applying this algorithm for all time steps yields a single trajectory for a whale that is a function of the stochastic movement model as well as the historical whale spatial density. The basic random walk could in some sense be said to be 'biased' by the local landscape conditions. One feature of the algorithm is that to obtain a single whale trajectory requires, at each time step, the generation of many (n) candidate location predictions from which a single one is chosen. However, since the movement model and the weighted resampling are computationally trivial, the overall computational burden should be minimal. The size of n is user-specified and must be large enough so that whale location predictions sufficiently populate the local space around the current position, allowing an appropriate particle to be chosen for the trajectory that properly responds to the historical whale spatial density (see Supplementary Material). To generate an ensemble of whale trajectories, or many individual tracks, multiple runs of the above algorithm would be undertaken (these could be run in parallel). Finally, note that this approach is a general one — it can be applied to any Markovian movement model of the form (1) and will converge to the target posterior. The sequential Monte Carlo sampler is discussed further in Section 4.

2.4. Whale movement response to underwater noise

The simulated whales' response to the sound field incorporates three components:

1. A biphasic dose–response function that informs the probability of a response to noise disturbance.
2. Directional horizontal movement away from the loudest noise in the region of the whale. This changes over time as noise source(s) and the whales move.
3. Duration of behavioral disruption post-disturbance that affects directional persistence. The strength of the behavior changes decreases with time as behavior reverts to baseline according to an exponential decay governed by a 'disruption' parameter.

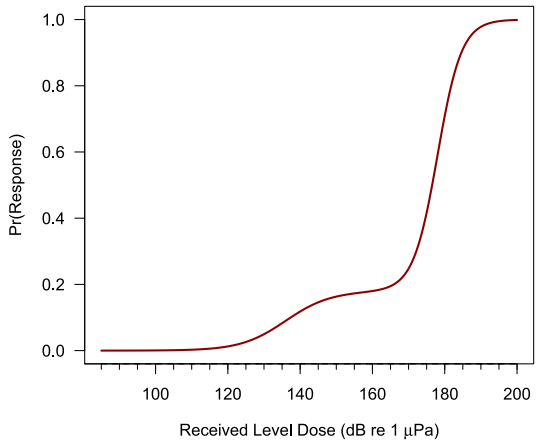

Fig. 1. Biphasic dose–response function for low-frequency (Mysticetes) whales, derived from (Finneran et al., 2017). The *x*-axis is the sound pressure level (SPL) or 'dose' received by a whale (dB re 1 µPa), and the *y*-axis is the probability of a behavioral response (BR) for a given SPL.

2.4.1. Biphasic dose–response function

Probability of behavioral response is modeled as a function of the acoustic dose of anthropogenic noise, quantified as the received sound level (RL). A biphasic functional relationship has been hypothesized (Ellison et al., 2012) whereby (i) at lower RLs the response is dependent on the pre-existing behavioral context of the whale, while (ii) at higher RLs a behavioral response is more likely and is more directly tied to RL. Combining these two modes of response and integrating over behavioral states leads to a biphasic function. This type of function has been fitted to experimental and observational data from multiple taxa, and used by the US Navy in its impact assessments (Finneran et al., 2017). Empirical data on fin whale responses to sonar are not yet available, thus the dose response relationship used here is borrowed from that of blue whales, a related Mysticete species in the same genus, Balaenoptera (Finneran et al., 2017). An example of the dose response functional form is shown in Fig. 1 (with modification possible once experimental/observational data become available). The probabilistic functional form is

$$Pr(Response) = \frac{p}{1 + 10^{(L_1 - Dose)h_1}} + \frac{(1-p)}{1 + 10^{(L_2 - Dose)h_2}} \quad (5)$$

where $Dose$ is the received sound pressure level (SPL, in dB re 1 µPa) of broadband noise, p is the proportion of the curve comprising the first (lower dose) phase, L_1 is the broadband SPL at the midpoint (inflection point) of the first phase, L_2 is the broadband SPL at the midpoint (inflection point) of the second phase, h_1 is the slope of the first phase where smaller values correspond to lower contextual response, and h_2 is the hill slope of the second phase. This model is a generalization of the monophasic models previously developed and applied in this context, e.g., Antunes et al. (2014) and Miller et al. (2014). Other forms of dose–response function than those of mono- and bi-phasic forms could readily be used. We refer the reader to the Supplementary Material for additional information on this function.

2.4.2. Directional response to noise

Suppose there is a received level sufficiently loud to trigger a behavioral response (BR) via Eq. (5) at time t at the animal's location, $\boldsymbol{x}_t$. The movements of the whale to next location $\boldsymbol{x}_{t+1}$ are modeled as having a behavioral response such that it moves in a direction 180° away from the maximum sound source. This angle is described by the 2×1 unit vector $\theta_{sound(t)}$ containing the easting and northing vector components. The magnitude of the movement is taken to be identical to the horizontal displacement computed by the movement model in the absence of any noise effect. This corresponds to a step size dictated by the realization of ϵ_{t+1}, and is the Euclidean distance between $\boldsymbol{x}_t$ and $\boldsymbol{x}_{t+1}$, or $\|\boldsymbol{x}_{t+1} - \boldsymbol{x}_t\|$. At the new position, $\boldsymbol{x}_{t+1}$, at time, $t+1$, if the sound level is still sufficient to trigger another behavioral response then the procedure continues by moving 180° away from the 'new' direction of maximum sound source, $\theta_{sound(t+1)}$ with the distance $\|\boldsymbol{x}_{t+2} - \boldsymbol{x}_{t+1}\|$. Goldbogen et al. (2013) found whales responded with directional travel away from the sound source when exposed to playbacks of military sonar. In some cases, whales have been shown to increase speed in response to sonar (e.g., DeRuiter et al., 2013), and this could readily be incorporated if desired.

2.4.3. Disruption of behavior: time to revert to baseline behavior after a behavioral response

Once a behavioral response occurs, then the post-disturbance movement process gradually reverts back to that of the disturbance-free movement model. The rate at which this happens is governed by a parameter α^{τ}, where τ is the number of time steps (or dives) since the most recent behavioral response occurred, and α is the 'disruption' parameter, $(0 \leq \alpha \leq 1)$. Since it is only the direction of movement that is changed, the post-disturbance direction at time step τ, θ_t, is computed as

$$\theta_t = \alpha^{\tau}\ \theta_{sound(t)}\ +\ (1 - \alpha^{\tau})\ \theta_{movement(t)} \quad (6)$$

where the right-hand-side of (6) represents a weighted average of the directions $\theta_{sound(t)}$, (180° from the time-varying sound source at time t), and $\theta_{movement(t)}$ (the time-varying direction given by the stochastic movement model at time t). The relative weighting changes with time since disturbance, τ, and at each step the direction of maximum sound is re-evaluated (updated for movements by both the whale and sound source). If no behavioral responses occur such as when the noise source ceases, the whale remembers the direction of maximum sound from the most recent $\theta_{sound(t)}$. The 'disruption' parameter dictates the rate at which this behavior returns to baseline such that when $\alpha = 0$ there is no change in behavior from past disturbance, and when $\alpha = 1$ the whale never returns to its baseline behavior. Note that while the above procedure is explained in terms of a single noise source, the ideas are generalizable to different dose response functions, multiple behavioral responses, different magnitudes of response, and multiple simultaneous moving noise sources.

2.5. Applications

We illustrate the movement model through two applications: (i) an idealized example that highlights the features of the simulation tool using a synthetic historical whale spatial density and a synthetic sound source, and (ii) a realistic case study focused on the consequences of acoustic disturbance on a population of fin whales to the west of the Southern California Anti-Submarine Warfare Range (SOAR, located west of San Clemente Island, Southern California). The simulation model and all analysis is written in R (R Core Team, 2020).

2.5.1. Generic whale movement model with synthetic noise: an idealized application

We demonstrate the movement model for a generic whale moving through a region where a bimodal distribution is imposed that reflects local habitat quality and specifies the historical whale spatial density. This idealized scenario simulates one year of whale movement both in the absence and presence of noise disturbance. For simplicity, we fix the bathymetry of the idealized region to be deeper than the deepest DTAG dive registered for tagged fin whales tagged in this region (i.e., > 359 m). The purpose here is to demonstrate that the particle filter algorithm described in Section 2.2 can be used to construct simulated whale tracks that reflect the historical whale spatial density, as well as how the introduction of noise affects the movement.

Dive duration is determined by drawing randomly from a distribution derived from fin whale DTAG data (see Supplementary Materials

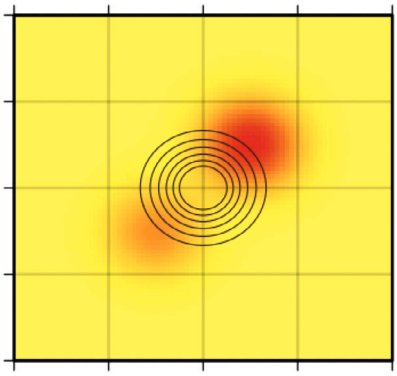

Fig. 2. Set up for the idealized case. The colors show the historical whale spatial density in the region where darker red indicates higher probability of a whale presence. Also shown are underwater noise contours where each line represents 20 dB difference in amplitude between 100 dB (the outer contour line) and 200 dB (the innermost/smallest contour line), the 0 to 1 range of the biphasic dose–response function in Fig. 1.

for more details on the DTAG data). The dive step variance, σ_t^2, is then scaled to the dive duration such that the characteristic displacement is $\sigma_t = speed \times dive\,duration$) where the $speed$ is taken as 1 m/s and represents a typical surface speed. Once σ_t^2 is determined, we follow the movement sampler of Section 2.2 with a sample size of $n = 30$ (See Supplementary Material for an analysis of sensitivity to the number of particles, n). Note that we incorporate the additional constraint of having movement displacements such that they cannot exceed the maximum speed for fin whales (assumed to be 7.7 m/s, or 15 knots; Aguilar and García-Vernet (2017).

Fig. 2 shows the synthetic historical whale spatial density constructed as a mixture of two bivariate normal distributions. Also shown in Fig. 2 is a synthetic, isotropic noise field centered at (0,0). The sound pressure level contours in Fig. 2 correspond to 20 dB increments of broadband noise between 100 and 200 dB re 1 μPa. The smallest circle corresponds to 200 dB isocline, which implies a 100% chance of the simulated whale responding to noise at that location using the dose–response function of Fig. 1. Similarly, outside the biggest circle, received levels are below 100 dB corresponding to a 0% chance of eliciting a behavioral response. The sound source is always on for the duration of this idealized simulation.

We explored the following scenarios as numerical experiments:

1. *Whale trajectory in the absence of underwater noise*. The simulated whale trajectories are based only on the random walk model and responding to the historical whale spatial density as dictated by the particle filter.
2. *Whale trajectory in the presence of continuous underwater noise, weak disruption*. Simulation of whale movement using both the historical whale spatial density and the imposed underwater noise field. The disruption parameter of (6) is set as $\alpha = 0.5$ which implies a relatively short disturbance period and less directional persistence away from the local noise source.
3. *Whale trajectory in the presence of continuous underwater noise, strong disruption*. As above, but with $\alpha = 0.95$ implying a longer time before behavior returned to baseline after noise disturbance.

For each of the three numerical experiments, we summarize a one year whale trajectory with the resultant whale density function derived from the simulated trajectories, called the utilization density. This uses kernel-smoothed density estimation (Worton, 1989), and we assume a Gaussian kernel and select the smoothing bandwidth as recommended by Venables and Ripley (2002). This creates a map of the habitat utilization as dictated by the movement model, the historical whale spatial density and the noise field.

2.5.2. Fin whale response to naval sonar in southern California: a case study

In this application, we investigate the consequences of an extended period of naval sonar events on a population of fin whales in the waters off Southern California. This synthetic scenario consists of a single naval destroyer equipped with a surface-ship mid-frequency sonar ('53C'). We use an available regional fin whale density surface to bias the random walk towards preferred habitat using our movement sampler (Becker et al., 2016). The movement model uses realizations of dive behavior taken from tagged fin whales in the region and also accounts for local bathymetry (which limits dive depths) and coastlines (which act to constrain horizontal movement). Specifically, the following sources of data are used (more information about these data sources is given in Supplementary Material):

1. *Dive Data*. We incorporate the vertical component of whale habitat through the dives logged on animal tagging devices (e.g., DTAGs). Using tag data, we determine the relative amount of time spent at each 10 m depth interval, as well as the total dive duration and surface time of each dive. These dive duration set the displacement magnitude σ_t^2 (Eq. (2)) as in the idealized example. The realized displacement is conditional on the horizontal movement not exceeding the species' maximum swim speeds.
2. *Historical Whale Spatial Density*. We use the density surface of Becker et al. (2016) (Fig. 3) to bias the random walk towards preferred habitat according to the movement sampler.
3. *Noise Field*. We incorporate the estimated received level (RL) fields (Margolina et al., 2018) from a typical single-ship naval 53C sonar event to the east of the SOAR region at 5-minute time resolution. We use the NSPE (Navy Standard Parabolic Equation) model to describe transmission loss from the vessel position (sound source) along discrete bearings such that each 10 m depth 'slice' of RL is estimated as a sound map; the 20 m depth bin is shown in Fig. 3C (more details on the NSPE model can be found in the Supplementary Material). A whale's received level is determined by matching the transmission loss model prediction to the depth interval where the whale spends the most time during a dive. The temporal sonar sound production regime is based on data provided by the US Navy on hourly detections of Navy sonar at the nearby SOAR range for the two years 2014 and 2015. This disturbance regime is proposed only as a demonstration — we do not suggest that this level is applicable to the disturbance regime in the region. The duration of each sonar event is simulated with a gamma distribution (shape 1.845, rate 0.698) with mean of 2.64 h. The time between each sonar event is simulated using a gamma distribution (shape 0.561, rate 0.02) with mean of 27.86 h, corresponding to 272 naval sonar events per year. Overall, the expected percent of days with no sonar is 48%.
4. *Bathymetry*. The simulated whales' dive depths are constrained not to exceed the local depth, which can be an important constraint in shallow waters. Bathymetry at resolution of 3-arc second (~ 90 m) from the National Geophysical Data Center was used (US Coastal Relief Model bathymetry; www.ngdc.noaa.gov/mgg/bathymetry/relief.html) (Fig. 3A).

In this application, we follow a population of 1176 fin whales for one year. This number comes from integrating the regional density surface used to predict the number of fin whales from the 2-D log linear model reported in Becker et al. (2016). We simulate movement of each individual in the horizontal and vertical dimensions with dive-by-dive resolution in the presence of multiple exposures to point sources of underwater sound. Each whale's trajectory corresponds to one year of animal movement and tracks each individual's history of disturbance. Within a year, for each naval sonar event, the whale is assigned a unique threshold noise value above which the whale has a behavioral

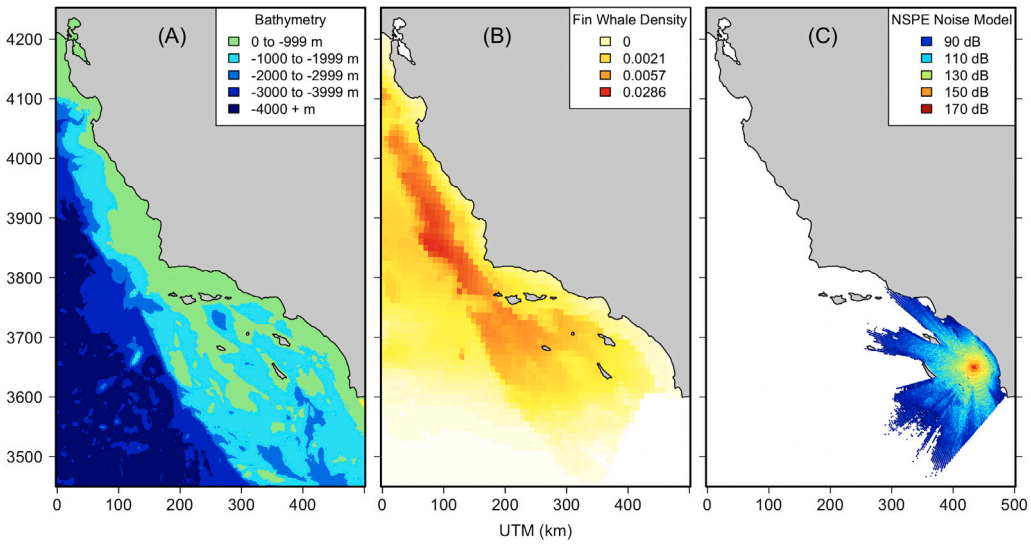

Fig. 3. Panel A: Bathymetry of the coastal Southern California region of interest. Panel B: Species distribution model surface of Becker et al. (2016) used as historical whale spatial density. Panel C: Estimated received level of sound in the 10–20 m depth bin for a single position of the naval sonar, dB re 1 μPa (C).

response. This response threshold is randomly generated from the dose–response function by treating it as a cumulative distribution function. If the estimated received level at the horizontal and vertical location of the whale exceeds this response threshold, the whale responds.

We apply the dose–response function (Fig. 1) at each dive but count only one BR per naval sonar event. Multiple events that elicit a response for an individual whale can be accumulated across time. If a whale has one or more BR across a time period, the fin whale's movement trajectory is then a mixture of the movement model and its unique exposure history and its memory thereof. A schematic is presented in Fig. 4.

We ran two numerical experiments of one year duration on the population of 1176 whales, but with different 'disruption' parameters. The first experiment describes a population of fin whales whose movement is disrupted, on average, for 20 min ($\alpha = 0.05$) post disturbance. We assume 48% of days have naval sonar events, or 272 events across 365 days. The second experiment similarly describes a population of 1176 fin whales with the same regimen of naval sonar events but where this population retains a disruption memory on average of three days ($\alpha = 0.99$; as reported for behavioral response of beaked whales by McCarthy et al., 2011). As with the idealized example, we map the ensemble of whale trajectories using kernel density estimation to create a distribution surface.

3. Results

3.1. Results for idealized case with synthetic noise

The first application details the simulated horizontal movement of an individual whale in an idealized setting. Fig. 5 shows the results from the 3 different scenarios: (1) whale track without noise (Fig. 5A–C); (2) whale track with noise and weaker disruption ($\alpha = 0.50$; Fig. 5D–F); and (3) whale track with noise and stronger disruption ($\alpha = 0.95$; Fig. 5G–I). For each scenario, the left column of Fig. 5 provides the reference historical whale spatial density and the noise field (if present), the middle column is the simulated whale trajectory and the right column is the kernel density reconstruction of the whale density from the simulated tracks, which we term the utilization, or posterior, density surface.

The results from the noise-free scenario (top row of Fig. 5) demonstrates that the movement trajectory is an effective sampler of the underlying bimodal historical whale spatial density. The whale track in Fig. 5B shows that in the absence of noise the simulated whale moves between the modal regions of the density surface and is faithful to their relative probabilities (note that more opaque red indicates more time spent in an area), while avoiding areas that have low historical whale spatial density. The kernel density estimate (Fig. 5C) matches well the true underlying historical whale spatial density (Fig. 5A).

The introduction of noise in addition to the historical whale spatial density alters the movement trajectories and the utilization density (Table 1). When the noise is sufficiently loud to elicit a behavioral response from the whale, the trajectory moves 180° away from the sound source in the first interval, with a decay in directional persistence proportional to its sensitivity or 'disruption' parameter that defines how long before an individual returns to baseline behavior post-disturbance. This results in directed movement away from the noise source and, given that the sound level of 200 dB re 1 μPa corresponds to a probability of a behavioral response equal to 1, it results in a region of zero occupancy (no whale tracks) near the origin. The sound source also has the effect of blocking the transiting of the whale between the two areas of preferred habitat.

This region of whale exclusion is seen for both noise scenarios in both the trajectories (Fig. 5E, H), as well as in the kernel density estimate of the whale utilization density (Fig. 5F, I). Parts of this central region with the highest noise amplitude would have been an area of preferred habitat and have more movement tracks in the absence of the noise disturbance. Outside of the central acoustic exclusion zone, in regions with moderate received levels, there is also a reduced tendency to use this habitat (Table 1, cols. 3 and 4). This is combined with a general tendency to preferentially use the eastern half of the domain. The noise source region thus not only acts as an exclusion zone, it also acts as a partial barrier for the simulated movement. In the case of low disruption parameter, the simulated whale initially moves to the preferred habitat to the northeast and then spends most of its time there, but is able to transit to the preferred habitat in the southwest by going south of the sound source (Fig. 5E). With a large disruption parameter, the whale is essentially fully blocked from going to the preferred habitat in the southwest. Whale movement preferentially tends toward the high historical whale spatial density region in the northeast and eastward since strong disruption means more persistence in moving away from the sound source (Fig. 5H, I).

The details of habitat utilization are also affected by the acoustic disruption. The role of the disruption parameter α can be ascertained

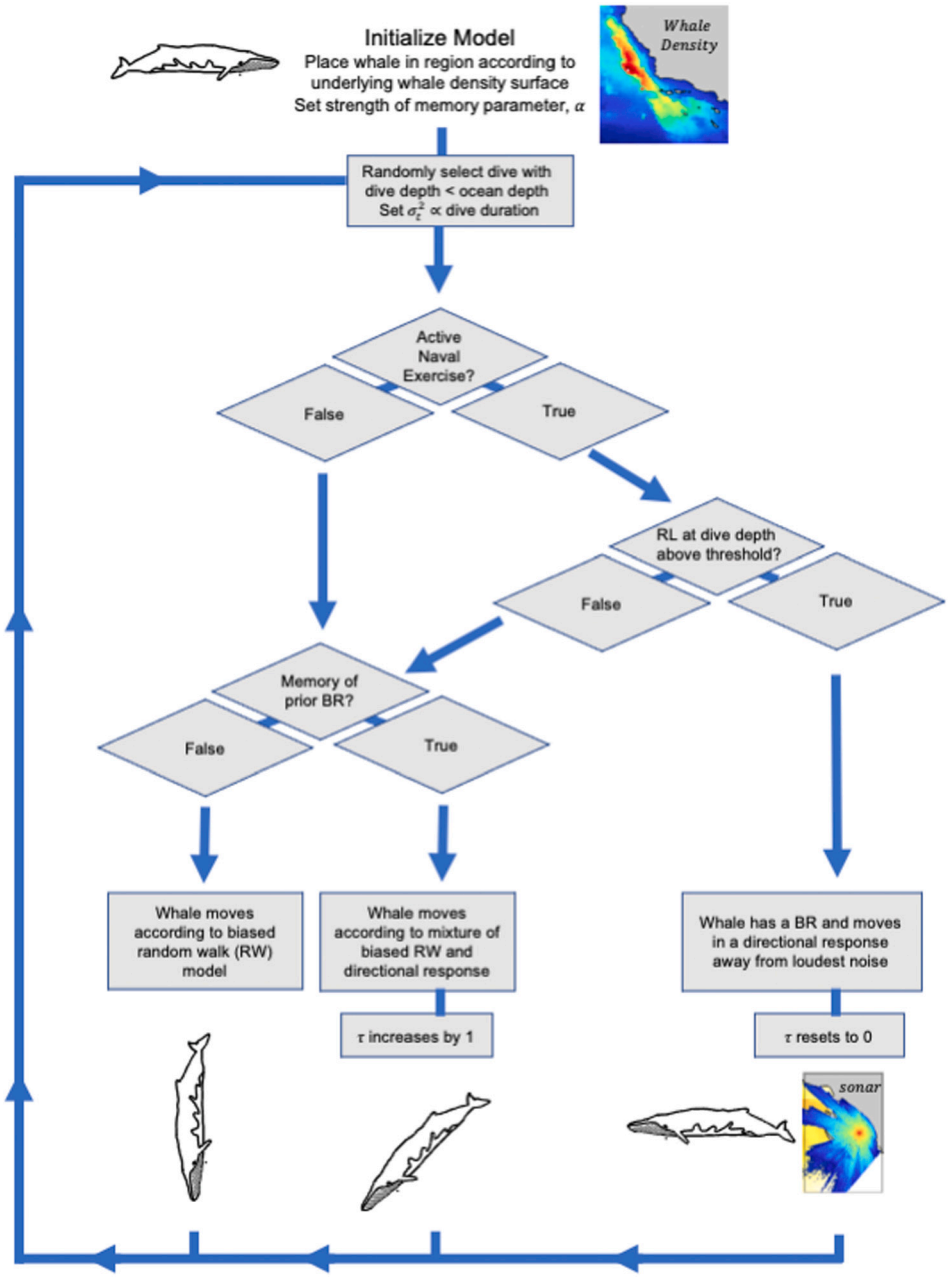

Fig. 4. Conceptual diagram describing the three movement scenarios: whale movement in the absence of noise, movement in response to prior disturbance, and movement mediated through a behavioral response to excessive received level of noise. Here, 'BR' stands for behavioral Response to naval sonar, and τ represents the dive (time) steps since the most recent BR, and t corresponds to the dive steps across the monitoring period and varies from 1 and T (the number of dives in a year).

Table 1
The percentage of dives displaced relative to the noise contour that corresponded to a 5% probability of a behavior response (BR; 130.13 dB re 1 μPa) and 50% probability of a BR (176.52 dB re 1μPa). The first row of this table corresponds to the 130.13 dB contour shown in Fig. 5 E-H. Dive displacement is relative to the number of dives that occurred in the absence of noise. The rows in this table correspond to different dose–response received level thresholds, whereas columns 3 and 4 correspond to displacement with different disruption parameters (α = 0.50, 45-minute behavior disruption, col. 3; α = 0.95, 10-hour behavior disruption, col. 4).

Probability of experiencing a BR	Received Level (dB re 1 μPa)	Relative % dives displaced (α = 0.50)	Relative % dives displaced (α = 0.95)
P(BR) = 0.05	130.13 dB	81.4%	92.8%
P(BR) = 0.50	176.52 dB	96.5%	98.3%

by contrasting the weaker disruption scenario (α = 0.5) to the stronger disruption (α = 0.95) scenario. In the stronger disruption scenario, the tracks are more broadly spread out over a larger region (Fig. 5E) as compared to the weaker memory case (Fig. 5H), and the corresponding density surface is more diffuse (Fig. 5F and I). The memory effect also influences the number of noise-induced behavioral responses (BRs that the whale is subjected to: the strong memory case had 2.5 times lower number of BRs compared to whales that had shorter behavior disruptions from disturbance when evaluated across a year of continuous sound exposure (1342 BRs for α = 0.5 vs. 542 BRs for α = 0.95). This corresponds to 2.5 times fewer dives at BR inducing exposure levels when disturbance memory is stronger as whales tend to be more distant from the sound source. While whales with strong memory have fewer behavior responses, these whales also spend more time in less-favorable habitat.

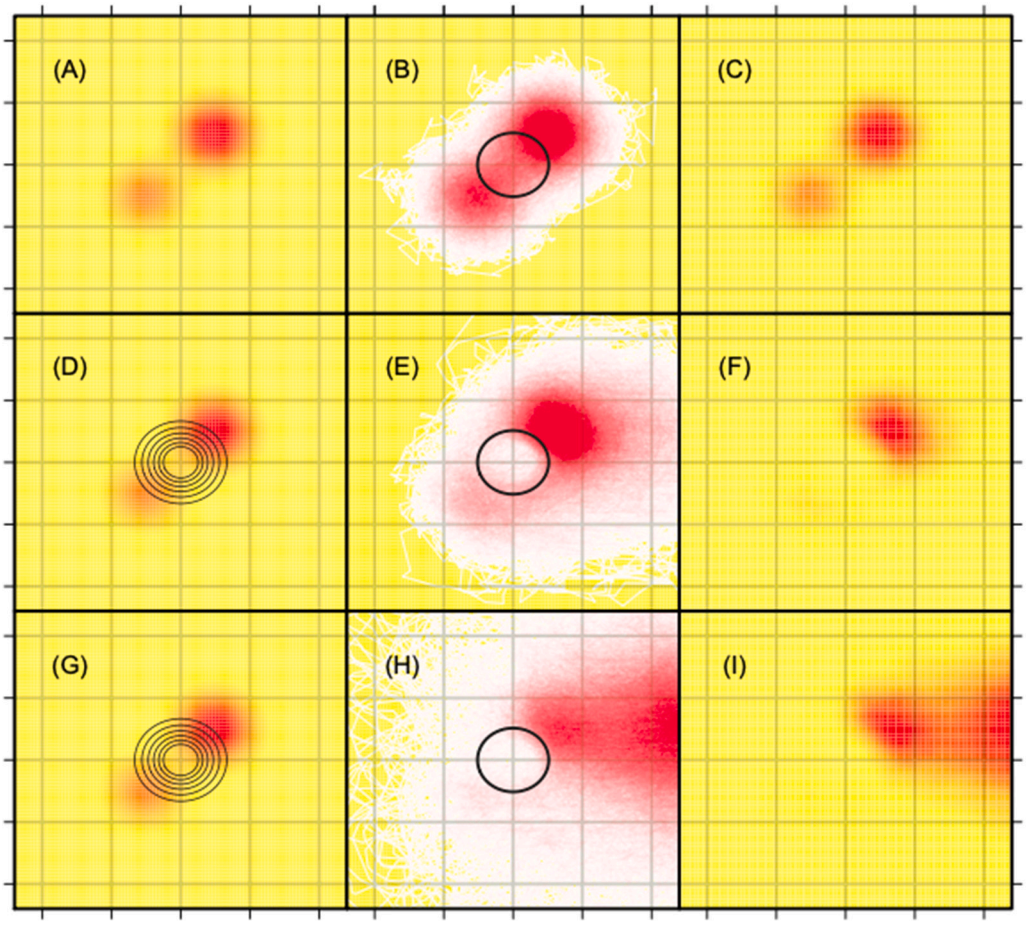

Fig. 5. Results from the idealized application. Row 1, Panel (A): a synthetic bimodal historical whale spatial density in the absence of noise with low densities appearing yellow and higher densities appearing red. Panel (B): the forward simulator of whale trajectories based only on the movement model for one year. Simulated whale dive locations are colored white, the track line is transparent red, with more overlapping locations rendering tracks darker red. Panel (C): Two-dimensional kernel density estimation of whale utilization density surface. Row 2: Panels (D, E, F): the same as Row 1 except now with a stationary noise source denoted by the concentric gray contours, and disturbed whales quickly returning to baseline movement behavior ($\alpha = 0.50$). Row 3: same as Row 2, but taking longer to return to baseline post-disturbance ($\alpha = 0.95$). The circles in panels B, E, and H correspond to the 130.13 dB re 1 μPa contour where received levels inside this circle are ≥ 5% likely to elicit a BR from a pseudo-whale based on the biphasic dose response of Fig. 1 and see Table 1.

3.2. Results from fin whale case study in Southern California

This application simulates a population of fin whales off the coast of southern California exposed to noise from naval sonar. The individual whale trajectories of 1176 fin whales across a one year time period are shown in Fig. 6(B) and (C). In the figure, each simulated track is partially transparent such that we see the aggregate of the population trajectories. Collectively, as with the idealized scenario, the yearly movement trajectories of the population of 1176 fin whales recreates the original historical whale spatial density as taken from Becker et al. (2016).

The southeastern region of Fig. 6 contains the subregion (in gray box) where the naval destroyer conducts a sequence of sonar events and exposes the population to received levels high enough to elicit a BR from a fin whale. This subregion is also depicted in Fig. 7. Whales in this subregion respond to the disturbance through their horizontal movement. As this subregion is not a significant hotspot for fin whales, the effect of naval disturbance on individual movement has less impact (than Fig. 5(C) vs. (F), (I)), and therefore is less influential on the aggregated population's habitat utilization. This pattern arises from the region hosting fewer whales and therefore, fewer opportunities for an overlap of whales and noise disturbance.

In Fig. 7, we show the naval sonar exposure field and the BR history for two identical populations of 1176 whales, differing only in their return time to baseline behavior after a disturbance. In both cases, 79 of the 1176 fin whales in the southern California region were affected by naval sonar events (Table 2). This means 7% of the population experienced a received level high enough to experience a behavioral response. Comparing the short disruption time before return to baseline behavior (Fig. 7B) to the long disruption time case (Fig. 7C) shows higher numbers and density of BRs in the short disruption case over the long disruption case. This means that whales that return to the area faster (returning to baseline movement behavior sooner) could have greater consequences from the same disturbance regime at the end of a year of monitoring. Specifically, in the short disruption case, there were a total of 328 BRs across the 79 whales with a response to the naval disturbance, i.e., 0.27 (95% C.I., 0.16, 0.44) BRs per whale per year. Comparatively, there were 198 BRs shared across the 79 whales when a longer disruption time occurs, i.e., 0.17 (95% C.I., 0.10, 0.25; Table 2).

At the individual dive level over the course of a year, the largest impact (most BRs) occurs when the return time to baseline behavior is short (smaller disruption parameter α) and the whale is exposed to threshold sound levels for 163 dives. When the return time is long (larger α), the maximum dives above threshold noise levels, fell to 39. This corresponds to four times fewer dives at BR inducing exposure levels largely due to whales being more distant from the sound source when the disruption parameter is greater. When translated to time, this corresponds to 15.3 h (95% C.I.: 2.36, 59.5 h) and 3.7 h (95% C.I.: 0.56, 14.2 h) of time exposed to noise above the BR threshold for the

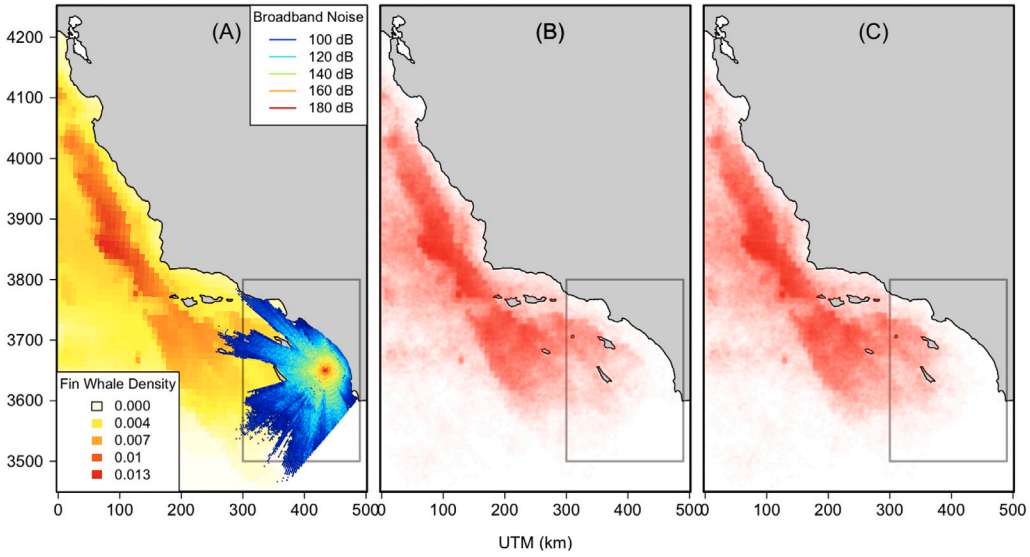

Fig. 6. Panel (A): the historical whale spatial density of fin whales superimposed with the naval sonar noise field showing all received levels ≥ 100 dB (below which the dose is too low to elicit a BR; Fig. 1). See Fig. 3 for separated panels for noise and whale density. Panels (B) and (C) depict the translucent pathways of a population of whales with disruption parameters informing the time before whales revert to baseline movement behavior: 20 min post-disturbance response (B) and 3 days (C). The gray rectangle in the panels corresponds to the image area of Fig. 7.

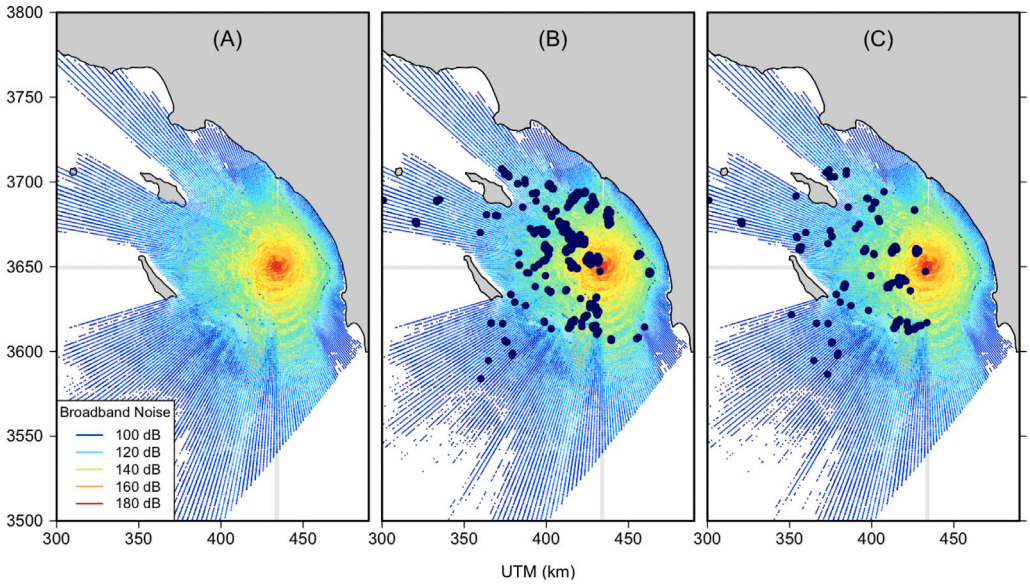

Fig. 7. Panel A: The sonar noise field in the sub-region of high noise. Panel B: the location and relative number of BRs when the disturbance time to baseline behavior is 20 min. Panel C: same as panel B but disturbance time is 3 days.

Table 2
Behavioral response (BR) events for a population of 1176 fin whales monitored over 365 days for exposure to naval sonar events. 95% confidence intervals are derived through bootstrapping individual tracks within the simulation.

Disruption parameter	Sum of BRs in population per year	Avg. number of BRs per whale per year	Max. number dives above threshold for a single whale
0.05	328	0.27 (0.16, 0.44)	163
0.99	198	0.17 (0.10, 0.25)	39

short and long changes in behavior cases, respectively. Many of these individual dive-level impacts are logged within the same naval sonar exercise. That is, the 163 and 39 dives above the BR noise thresholds occurred during just five sonar exercises. As the convention is to count a maximum of one BR per whale per naval exercise (Finneran et al., 2017), the range of BRs for a single whale is between 0 and 5. It is worth remembering, however, that higher values of the disruption parameter means a longer period of displacement, even if in aggregate it means fewer BRs.

4. Discussion

In this study, we have presented a framework for simulating marine animal movement. Its novelty is the following: (i) a flexible movement

simulator (sampler) wherein a stochastic movement model adapts to a pre-defined whale density surface using a sequential Monte Carlo algorithm (particle filter); (ii) inclusion of dive information in the forward simulator to control the magnitude of the displacement variance term and set the step size, thereby linking the horizontal and vertical movement dynamics; (iii) inclusion of a probabilistic behavioral response to sound using a biphasic dose–response curve that operates as a stochastic element within a movement model to trigger compensatory movement in response to disturbance; (iv) incorporation of short and long lasting behavior changes in response to sound-induced disturbance that controls the time-scale for reversion of movement to the disturbance-free case; and (v) realistic application to the fin whale population off southern California over biologically meaningful lengths of time (one year in our experiment). For this latter targeted application to naval sonar exposures, we demonstrated how movement histories and sound exposure at-depth for each track over an entire year can be summarized, thereby establishing the means to infer the impacts of cumulative disturbances on vital rates.

This movement modeling framework is general and flexible. It allows for incorporation of any stochastic movement model (e.g., continuous-time, or discrete-time with any time step). Rule-based alterations to movement were used to deal with the behavioral response to sound exposure and coastline avoidance. One novelty was to introduce a sequential Monte Carlo sampler that allows for movement realizations to be generated that are influenced by the historical whale spatial density. Most existing movement simulation frameworks provide a means to sample from a pre-defined known whale distribution that could be derived from a sighting data or a species distribution model (e.g., AIM, Frankel et al., 2002; SAFESIMM, Donovan et al., 2012; 3MB, Hauser, 2006; NAEMO, Blackstock et al., 2018). Michelot et al. (2019a,b) also treat this problem by proposing a Markov Chain Monte Carlo sampler whose target distribution is the historical whale spatial density (there called a resource selection function) with an emphasis on identifying movement models for which this feature holds. In fact, the random walk model of this study (in the absence of sound and coastline effects) corresponds to their 'local Gibbs over irregular sample intervals' whose long-run distribution is the historical whale spatial density.

Sequential Monte Carlo samplers are a flexible class of samplers based on forward kernels (movement models) and importance sampling, and offer a viable and, in some cases, superior alternative to Markov chain Monte Carlo samplers (Del Moral et al., 2006). Our sequential Monte Carlo sampler yields a movement generator faithful to the underlying historical whale spatial density surface, with the flexibility to also alter movement in response to coastlines, bathymetry, oceanographic fields, prey distributions, and underwater sound disturbance. It was demonstrated that when excessive noise is present, the movement of whales differs from the historical whale spatial density, reflecting changes in animal behavior in response to noise disturbance and the duration of response to that disturbance. It offers an alternative to the potential function approach (Brillinger, 2010) wherein movement trajectories are altered through imposed fields of attraction or repulsion.

We explored application of the movement simulation framework through two case studies: one idealized, and the other based on southern California fin whales. The idealized study illustrates the basic setup as well as how the simulator performs for a simple and intuitive situation. The more realistic application to fin whales with exposure to naval sonar provides an illustration of how the framework can be used to understand the cumulative effects of underwater sound over a biologically meaningful period of time. We were able to show that the consequences of a single disturbance are a function of how loud the received level at the whale's location, where the whale is relative to its preferred habitat when it is disturbed, and how long a whale takes before returning to a 'pre-disturbance' state. Over the one year time period, the movement framework links multiple disturbance events to individuals in a population that are repeatedly affected leading to a potential means to assess impacts on vital rates. That is, by examining the cumulative consequences of multiple naval sonar exercises in an animal's home range, we can look at energetic consequences of sound exposure.

In the fin whale case study, we observed some individuals being exposed more due to their proximity to the sonar exercises. If the consequence of disturbance can last up to 3 days (McCarthy et al., 2011), and BRs happen repeatedly to the same whale, then lower survival and breeding rates are likely consequences (Pirotta et al., 2018). In this case study, the locations of the naval sonar exercises did not overlap with a high density region of fin whales. Had the naval exercises overlapped more with high whale density regions, the consequences would likely have been greater. We would expect higher numbers of dives at received noise levels above the BR threshold, potentially eliciting more BRs and causing more fin whales to be excluded from preferred habitat for longer. If such responses were observed in many individuals, there would be a potential for impacts on fin whale population vital rates. As the simulated sonar used in our case study overlapped a low whale density area, and in reality it is unlikely that one exercise would represent the spatial extent of a year's worth of sonar exercises, it may be of interest to the US Navy to repeat this experiment with a more realistic set of spatial and temporal locations.

For our individual based model we made a series of assumptions and decisions using a bottom-up approach (in the sense of Grimm, 1999). Several of these necessarily simplify the underlying ecology. For example, simulated animals were assumed to move independently of each other. In many cases, animals are known to live in groups. This could most readily be included in the simulations by assuming that animal locations are, instead, group locations, and simulating a random group size. If further refinement were needed, the animal location could instead be considered to be the center of a group, with individuals displaying an attraction to this group center (e.g., Langrock et al., 2014). Another reason for non-independence is that many species live within home ranges within a larger population distribution. In this case, density surface model could be used to simulate a different home range center for each animal, and an individual density surface could then be generated for each animal, for example based on a bivariate normal distribution centered on its home range center. This would then be used instead of the population-level density surface to bias the animal movement model, so that the animal would tend to remain within its home range.

The movement of animals almost certainly deviates from the assumptions of this movement model, but we can use information about the characteristics of movement paths from real animals to derive better predictions of encounter rates with naval disturbance. That is, with the wealth of information from satellite tagging data we could create a more realistic movement model than a random walk, and have animals cue off of environmental and oceanographic features, or set movement model parameters to reflect behavioral state (e.g., foraging vs. traveling). Additionally, uncertainty could be incorporated on model inputs. For example, different whales could be given different dose–response functions reflecting permanent differences in responsiveness; uncertainty in the density surface could be incorporated through multiple simulations, each sampling from the possible range of inputs. Output uncertainty could then readily be quantified. We stress, however, that considerable complexity and understanding can be made using straightforward assumptions about movements (e.g., Nabe-Nielsen et al., 2013, 2014, 2018). The framework is a highly flexible, and similar approaches have yielded considerable insight about spatial patterns with and without disturbance (Nabe-Nielsen et al., 2018; Warwick-Evans et al., 2018). Our study offers opportunities for combining theory with data and to improve our understanding of spatial dynamics and naval impacts (Grimm, 1999).

With this framework in place, we are now able to examine impacts of a time-series of exposures and what these imply for individuals in terms of impacts on vital rates. Towards this end, there are several

frameworks that could be applied, including an individual-based model that tracks food intake (Nabe-Nielsen et al., 2013), and a dynamic state-variable approach (McHuron et al., 2017) that examines how disturbance may alter vital rates over the course of a year (Pirotta et al., 2018). Our model, once calibrated and validated, should prove useful as part of a decision-support tool in combination with existing methods to estimate behavioral effects of accumulated sound exposure for on-going efforts to assess the aggregate consequences of anthropogenic sources of disturbance and develop mitigation measures for affected populations.

CRediT authorship contribution statement

Ruth Joy: Conceptualization, Methodology, Writing. **Robert S. Schick:** Conceptualization, Methodology, Writing. **Michael Dowd:** Conceptualization, Methodology, Writing. **Tetyana Margolina:** NSPE Model, Writing – review & editing. **John E. Joseph:** NSPE Model, Writing – review & editing. **Len Thomas:** Conceptualization, Methodology, Writing.

Declaration of competing interest

One or more of the authors of this paper have disclosed potential or pertinent conflicts of interest, which may include receipt of payment, either direct or indirect, institutional support, or association with an entity in the biomedical field which may be perceived to have potential conflict of interest with this work. For full disclosure statements refer to https://doi.org/10.1016/j.ecolmodel.2021.109798. Declaration of Interest Statement for : A Fine-Scale Marine Mammal Movement Model for Assessing Long-term Aggregate Noise Exposure.

This project was funded by the US Navy through an Office of Naval Research Marine Mammals and Biology Program Grant awarded to SMRU Consulting Ltd. via a subcontract to the University of St Andrews.

Acknowledgments

We thank the following people for insightful discussions during development of the models: Charlotte Jones-Todd, Enrico Pirotta, Glenn Gailey, Brandon Southall, Sarah Blackstock, Lisa Schwarz, Dan Costa, Catriona Harris and Cormac Booth. We thank Elizabeth Becker for providing the fin whale species distribution model, and Stephanie Watwood and Nancy DiMarzio for providing data on hourly detections of sonar on the SOAR range used as the basis for our noise field simulation. This work was funded by the US Office of Naval Research, grant number N00014-16-1-2858: 'PCoD+: Developing widely-applicable models of the population consequences of disturbance'; we thank the entire PCoD+ team for their support. Mike Dowd was supported by a Natural Sciences and Engineering Research Council of Canada Discovery grant. We are grateful to the two anonymous reviewers for their helpful comments and suggestions, leading to a better paper.

Appendix A. Supplementary data

Supplementary material related to this article can be found online at https://doi.org/10.1016/j.ecolmodel.2021.109798.

References

Aguilar, A., García-Vernet, Raquel, 2017. Fin whale: *Balaenoptera physalus*. In: Würsig, B., Thewissen, J.G.M., Kovacs, K.M. (Eds.), Encyclopedia of Marine Mammals. In: Encyclopedia of marine mammals, Academic Press.

Antunes, R., Kvadsheim, P.H., Lam, F.P.A., Tyack, P.L., Thomas, L., Wensveen, P.J., Miller, P.J.O., 2014. High response thresholds for avoidance of sonar by free-ranging long-finned pilot whales (*Globicephala melas*). Mar. Pollut. Bull. 83, 165–180.

Becker, E.A., Forney, K.A., Fiedler, P.C., Barlow, J., Chivers, S.J., Edwards, C.A., Moore, A.M., Redfern, J.V., 2016. Moving towards dynamic ocean management: how well do modeled ocean products predict species distributions? Remote Sens. 8 (149).

Blackstock, S.A., Fayton, J.O., Hulton, P.H., Moll, T.E., Jenkins, K., Kotecki, S., Henderson, E., Bowman, V., Rider, S., Martin, C., 2018. Quantifying Acoustic Impacts on Marine Mammals and Sea Turtles: Methods and Analytical Approach for Phase III Training and Testing. Naval Undersea Warfare Center Division Newport, Rhode Island.

Boyce, M.S., McDonald, L.L., 1999. Relating populations to habitats using resource selection functions. Trends Ecol. Evol. 14 (268–272).

Brillinger, D.R., 2010. Modelling spatial trajectories. In: Gelfand, A., Diggle, P., Guttorp, P., Fuentes, M. (Eds.), HandBook of Spatial Statistics. CRC Press, Boca Raton, Florida, USA, pp. 463–474.

Del Moral, P., Doucet, A., Jasra, A., 2006. Sequential Monte Carlo samplers. J. R. Stat. Soc. Ser. B Stat. Methodol. 68 (3), 411–436.

DeRuiter, S.L., Southall, B.L., Calambokidis, J., Zimmer, W.M.X., Sadykova, D., Falcone, E.A., et al., 2013. First direct measurements of behavioural responses by cuvier's beaked whales to mid-frequency active sonar. Biol. Lett. 9, 20130223. http://dx.doi.org/10.1098/rsbl.2013.0223.

Donovan, C.R., Harris, C., Harwood, J., Milazzo, L., 2012. A simulation-based method for quantifying and mitigating the effects of anthropogenic sound on marine mammals. In: Proceedings of Meetings on Acoustics, Vol. 17. pp. 1–8. http://dx.doi.org/10.1121/1.4772738, 070043.

Donovan, C.R., Harris, C.M., Milazzo, L., Harwood, J., Marshall, L., Williams, R., 2017. A simulation approach to assessing environmental risk of sound exposure to marine mammals. Ecol. Evol. 7 (7), 2101–2111.

Dowd, M.G., Joy, R., 2011. Estimating behavioural parameters in animal movement models using a state augmented particle filter. Ecology 92, 568–575.

Ellison, W.T., Southall, B.L., Clark, C.W., Frankel, A.S., 2012. A new context-based approach to assess marine mammal behavioral responses to anthropogenic sounds. Conserv. Biol. 26 (1), 21–28.

Fauchald, P., Tveraa, T., 2003. Using first-passage time in the analysis of area-restricted search and habitat selection. Ecology 84 (2), 282–288.

Finneran, J., Henderson, E., Houser, D., Jenkins, K., Kotecki, S., Mulsow, J., 2017. Criteria and Thresholds for US Navy Acoustic and Explosive Effects Analysis (Phase III). Technical report, Space and Naval Warfare Systems Center Pacific, SSC Pacific, San Diego, CA, p. 183.

Frankel, A.S., Ellison, W.T., Buchanan, J., 2002. Application of the acoustic integration model (AIM) to predict and minimize environmental impacts. In: OCEANS'02 MTS/IEEE, Vol. 3. IEEE, pp. 1438–1443.

Goldbogen, J.A., Southall, B.L., DeRuiter, S.L., Calambokidis, J., Friedlaender, A.S., Hazen, E.L., Falcone, E.A., Schorr, G.S., Douglas, A., Moretti, D.J., Kyburg, C., 2013. Blue whales respond to simulated mid-frequency military sonar. Proc. R. Soc. B 280 (1765), 20130657.

Gordon, N.J., Salmond, D.J., Smith, A.F., 1993. Novel approach to nonlinear/non-Gaussian Bayesian state estimation. In: IEEE Proceedings F (Radar and Signal Processing, Vol. 140. IET Digital Library, pp. 107–113, (2).

Grimm, V., 1999. Ten years of individual-based modelling in ecology: what have we learned and what could we learn in the future? Ecol. Model. 115 (2–3), 129–148.

Hauser, D., 2006. A method for modeling marine mammal movement and behavior for environmental impact assessment. IEEE J. Ocean. Eng. 31 (1), 76–81.

Hooten, M.B., Johnson, D.S., McClintock, B.T., Morales, J.M., 2017. Animal Movement: Statistical Models for Telemetry Data. CRC Press.

Jonsen, I.D., Myers, R.A., Flemming, J.M., 2003. Meta-analysis of animal movement using state-space models. Ecology 84 (11), 3055–3063.

Joy, R., Dowd, M., Battaile, B., Lestenkoff, P., Sterling, J., Trites, A.W., Routledge, R., 2015. Linking northern fur seal dive behaviour to environmental variables in the eastern Bering Sea. EcoSphere 6 (5), 75. http://dx.doi.org/10.1890/ES14-00314.1.

Kitagawa, G., 1987. Non-Gaussian state-space modeling of nonstationary time series. J. Amer. Statist. Assoc. 82, 1032–1063.

Langrock, R., Hopcraft, J.G.C., Blackwell, P.G., Goodall, V., King, R., Niu, M., Patterson, T.A., Pedersen, M.W., Skarin, A., Schick, R.S., 2014. Modelling group dynamic animal movement. Methods Ecol. Evol. 5 (2), 190–199.

Langrock, R., King, R., Matthiopoulos, J., Thomas, L., Fortin, D., Morales, J.M., 2012. Flexible and practical modeling of animal telemetry data: hidden Markov models and extensions. Ecology 93 (11), 2336–2342.

Margolina, T., Joseph, J.E., Southall, B.L., 2018. Brs sound exposure modeling tool: a system for planning, visualization and analysis. In: OCEANS 2018 MTS/IEEE Charleston. IEEE, pp. 1–4.

McCarthy, E., Moretti, D., Thomas, L., DiMarzio, N., Morrissey, R., Jarvis, S., Ward, J., Izzi, A., Dilley, A., 2011. Changes in spatial and temporal distribution and vocal behavior of blainville's beaked whales (mesoplodon densirostris) during multiship exercises with mid-frequency sonar. Mar. Mammal Sci. 27 (3), E206–E226.

McHuron, E.A., Costa, D.P., Schwarz, L., Mangel, M., 2017. State-dependent behavioural theory for assessing the fitness consequences of anthropogenic disturbance on capital and income breeders. Methods Ecol. Evol. 8 (5), 552–560.

Michelot, T., Blackwell, P.G., Chamaillé-Jammes, S., Matthiopoulos, J., 2019b. Inference in MCMC step selection models. Biometrics 76 (2), 438–447.

Michelot, T., Blackwell, P.G., Matthiopoulos, J., 2019a. Linking resource selection and step selection models for habitat preferences in animals. Ecology 100 (1).

Miller, P.J., Antunes, R.N., Wensveen, P.J., Samarra, F.I., Alves, A.Catarina., Tyack, P.L., Kvadsheim, P.H., Kleivane, L., Lam, F.P.A., Ainslie, M.A., Thomas, L., 2014. Dose–response relationships for the onset of avoidance of sonar by free-ranging killer whales. J. Acoust. Soc. Am. 135 (2), 975–993.

Morales, J.M., Haydon, D.T., Frair, J., Holsinger, K.E., Fryxell, J.M., 2004. Extracting more out of relocation data: building movement models as mixtures of random walks. Ecology 85 (9), 2436–2445.

Nabe-Nielsen, J., van Beest, F.M., Grimm, V., Sibly, R.M., Teilmann, J., Thompson, P.M., 2018. Predicting the impacts of anthropogenic disturbances on marine populations. Conserv. Lett. 11 (5), e12563.

Nabe-Nielsen, J., Sibly, R.M., Tougaard, J., Teilmann, J., Sveegaard, S., 2014. Effects of noise and by-catch on a danish harbour porpoise population. Ecol. Model. 272, 242–251.

Nabe-Nielsen, J., Tougaard, J., Teilmann, J., Lucke, K., Forchhammer, M.C., 2013. How a simple adaptive foraging strategy can lead to emergent home ranges and increased food intake. Oikos 122 (9), 1307–1316.

National Academies of Sciences, Engineering, and Medicine, 2017. Approaches to UnderstandIng the Cumulative Effects of Stressors on Marine Mammals. The National Academies Press, Washington, DC, http://dx.doi.org/10.17226/23479.

Parrott, L., Chion, C., Martins, C.C., Lamontagne, P., Turgeon, S., Landry, J.A., Zhens, B., Marceau, D.J., Michaud, R., Cantin, G., Ménard, N., 2011. A decision support system to assist the sustainable management of navigation activities in the st. Lawrence River Estuary, Canada. Environ. Model. Softw. 26 (12), 1403–1418.

Patterson, T.A., Parton, A., Langrock, R., Blackwell, P.G., Thomas, L., King, R., 2017. Statistical modelling of animal movement: an overview of key methods and a discussion of practical challenges. Adv. Statist. Anal. 101, 399–438.

Pirotta, E., Booth, C.G., Costa, D.P., Fleishman, E., Kraus, S.D., Lusseau, D., Moretti, D., New, L.F., Schick, R.S., Schwarz, L.K., Simmons, S.E., 2018. Understanding the population consequences of disturbance. Ecol. Evol. 8 (19), 9934–9946.

Preisler, H.K., Ager, A.A., Wisdom, M.J., 2013. Analyzing animal movement patterns using potential functions. Ecosphere 4 (3), 1–13.

R Core Team, 2020. R: A Language and Environment for Statistical Computing. R Foundation for Statistical Computing, Vienna, Austria, URL https://www.R-project.org/.

Southall, B.L., Finneran, J.J., Reichmuth, C., Nachtigall, P.E., Ketten, D.R., Bowles, A.E., Ellison, W.T., Nowacek, D.P., Tyack, P.L., 2019. Marine mammal noise exposure criteria: Updated scientific recommendations for residual hearing effects. Aquat. Mamm. 45 (2), 125–232.

Tyack, PL., Johnson, M., Soto, NA., Sturlese, A., Madsen, PT., 2006. Extreme diving of beaked whales. J. Exp. Biol 209, 4238–4253. http://dx.doi.org/10.1242/jeb.02505.

Venables, W.N., Ripley, B.D., 2002. Random and mixed effects. In: Modern Applied Statistics with S. Springer, New York, NY, pp. 271–300.

Warwick-Evans, V., Atkinson, P.W., Walkington, I., Green, J.A., 2018. Predicting the impacts of wind farms on seabirds: An individual-based model. J. Appl. Ecol. 55 (2), 503–515.

Whitford, M., Klimley, A.P., 2019. An overview of behavioral, physiological, and environmental sensors used in animal biotelemetry and biologging studies. Anim. Biotelemetry 7 (1), 1–24.

Whoriskey, K., Auger-Méthé, M., Albertsen, C.M., Whoriskey, F.G., Binder, T.R., Krueger, C.C., Mills Flemming, J., 2017. A hidden Markov movement model for rapidly identifying behavioral states from animal tracks. Ecol. Evol. 7 (7), 2112–2121.

Worton, B.J., 1989. Kernel methods for estimating the utilization distribution in home-range studies. Ecology 70, 164–168.